

Supplementary material

Characteristics of the Monsoon Low Pressure Systems in the Indian Subcontinent and the Associated Extreme Precipitation Events

Tresa Mary Thomas¹, Govindasamy Bala^{1,2} and Srinivas Venkata Vemavarapu^{1,3}

¹Interdisciplinary Centre for Water Research, Indian Institute of Science, Bangalore.

²Centre for Atmospheric and Oceanic Sciences, Indian Institute of Science, Bangalore.

³Civil Engineering, Indian Institute of Science, Bangalore.

Correspondence to: tresathomas@iisc.ac.in

S1. Automated Tracking Algorithm using Geopotential Criteria (ATAGC)

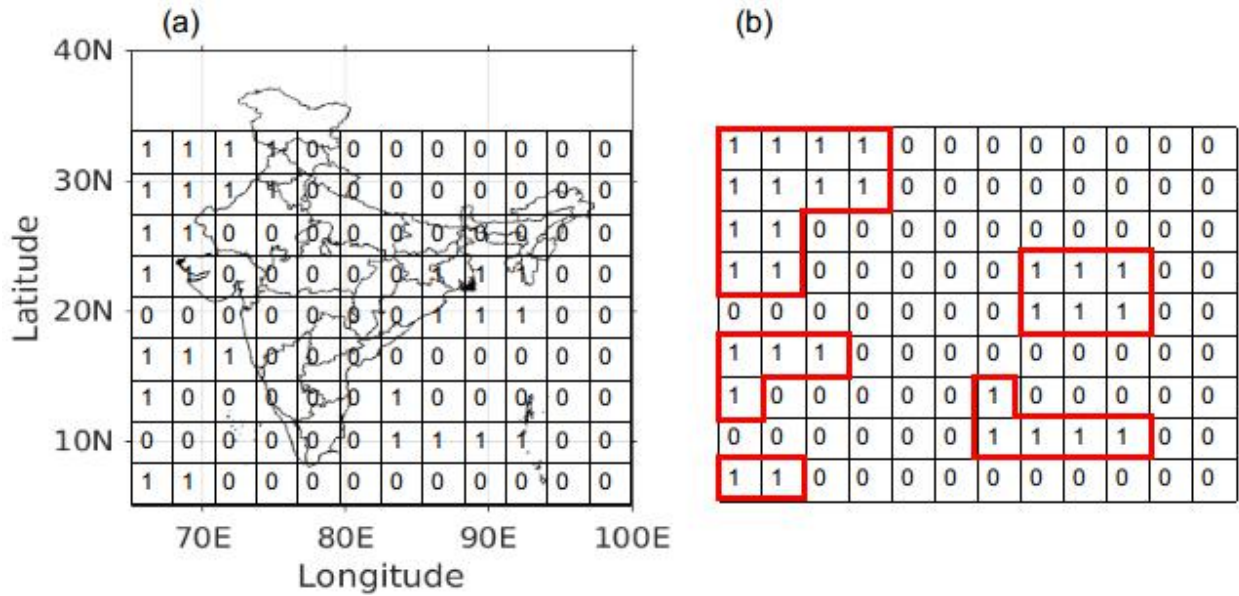


Fig. S1 Illustration of segmentation over (a) the study area comprising $0.75^\circ \times 0.75^\circ$ resolution grid. (b) result of application of segmentation for a typical time frame. If the value of relative vorticity is greater than α ($=0.5 \times 10^{-5} \text{ s}^{-1}$), the location is given a value 1, else it is assigned a value 0. Boxes in red represent uniquely identified object classes for the time frame using connected compound labeling algorithm

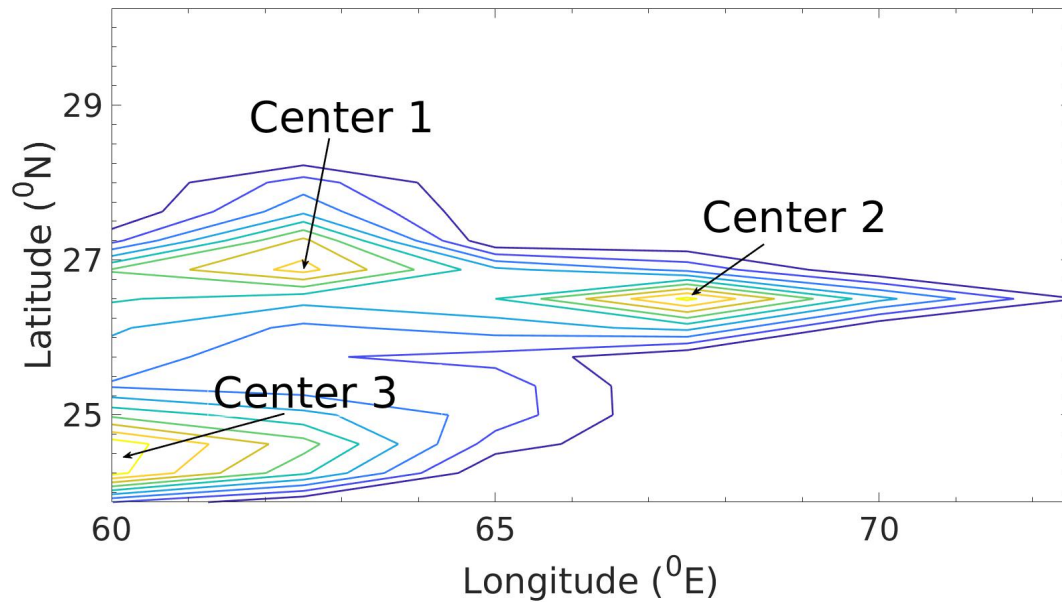


Fig. S2 Contours of relative vorticity inside an object class identified for a given time frame. Feature points are identified as relative vorticity maxima that are 3° apart from each other. In this illustration, 3 feature points are identified as indicated by the numbers

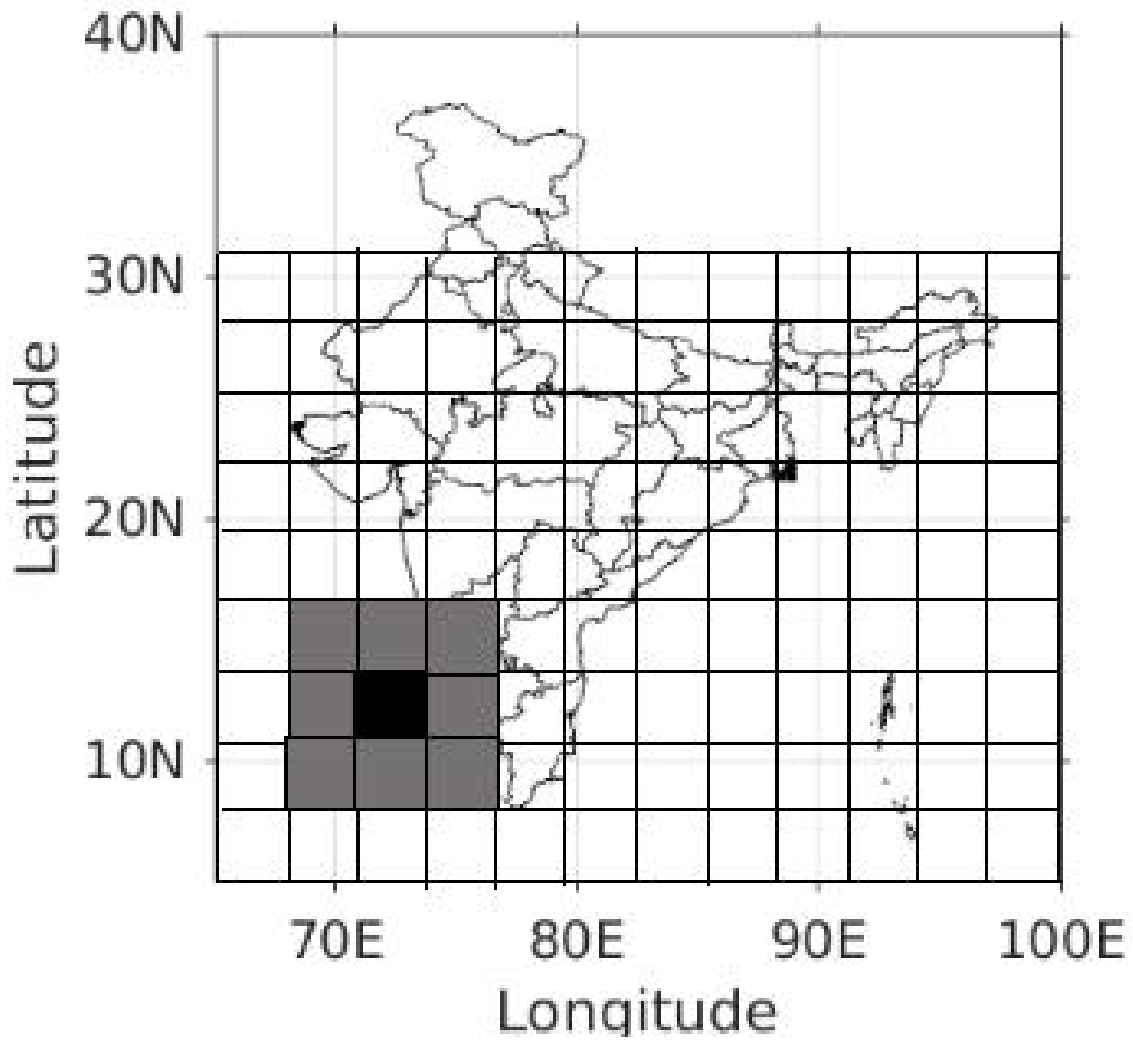


Fig. S3 Determination of Geopotential anomaly. Geopotential Anomaly at the location shown in black is determined by subtracting the mean of geopotential height values at the surrounding 8 locations (grey) from the geopotential height value at the black location. If the anomaly at a location is less than $-120\text{m}^2/\text{s}^2$, it is considered as a positive location

S2.1. Probability of Coincidence

The probability of coincidence (Blender and Schubert 2000) can be used to compare two sets of tracks. A track is defined by a set of T points, where each point t ($=1, \dots, T$) is represented by its latitude $\varphi(t)$, longitude $\lambda(t)$, and time $k(t)$. Let the first set of tracks be defined as $\varphi_1(t_1)$, $\lambda_1(t_1)$, $k_1(t_1)$, where $t_1=1, 2, \dots, T_1$. Similarly, let the second set of tracks be defined as $\varphi_2(t_2)$, $\lambda_2(t_2)$, $k_2(t_2)$, where $t_2=1, 2, \dots, T_2$. Spatio-temporal distance between the two tracks can be computed as,

$$D_{12}^2 = \frac{1}{T_1 T_2} (\sigma_{12}^2 - \frac{1}{2} (\sigma_{11}^2 + \sigma_{22}^2)) \quad (1)$$

where,

$$\sigma_{ij} = \frac{1}{T_i T_j} \int_0^{T_i} dt_i \int_0^{T_j} dt_j \left(\alpha \left([\varphi_i(t_i) - \varphi_j(t_j)]^2 + [\lambda_i(t_i) - \lambda_j(t_j)]^2 \right) + \beta [k_i(t_i) - k_j(t_j)]^2 \right) \quad (2)$$

where the weight function $\beta = \alpha U^2$ and $\alpha = 1$ and $U = 10$ m/s following Blender and Schubert (2000) and Praveen et al. (2015).

For any chosen track in set 1, the spatiotemporal distance with each track in set 2 is computed and the track for which the D^2 value is minimum is considered to be similar track in set 2. Distance of the identified similar track is then computed with respect to each of the tracks in set 1, and the track for which the D value is minimum is considered to be similar track in set 1. If that similar track is same as the track initially chosen in set 1, then the identified track in set 2 and the chosen track of set 1 are considered as identical tracks. The probability of coincidence of tracks in a given year is the ratio of number of identical tracks determined in that particular year to the total number of tracks observed in that year.

$$P_c = \frac{\text{Number of identical Tracks}}{\text{Total Number of Tracks}} \quad (3)$$

S2.2. Root mean squared Difference

The root mean square difference between the set of observations $x = \{x_1, x_2, x_3, \dots, x_n\}$ and $y = \{y_1, y_2, y_3, \dots, y_n\}$ is given as

$$RMSD = \sqrt{\frac{\sum_{i=1}^n (x_i - y_i)^2}{n}} \quad (4)$$

S3. Synoptic Activity Index (SAI)

SAI is an index to measure the LPS activity at a given location by accounting for the number and intensity of LPS at the given location (Ajayamohan et al. 2010). In this study, it is computed on a $3^{\circ}\times 3^{\circ}$ grid. The number of LPS observed at each location on a given day is counted. This number is then multiplied by a weighting factor (Table S1), which depends on intensity of the system, to arrive at their product. The weight for each category of the LPS is taken as the centroid of the wind speed range of that particular category of LPS as shown in Table S1. The product is summed over all the days of the monsoon season (June-September) to obtain an estimate of annual SAI for the $3^{\circ}\times 3^{\circ}$ grid. The sum of such annual SAIs is then computed and converted to mean SAI at daily scale for the monsoon season.

Table S1 Category of LPS and their associated wind speed range (in m/s), and weighing factor used for calculation of SAI for each category of LPS

Category of LPS	Wind Speed Range	Weighing Factor
Lows	0- 8.5	4.25
Depressions	8.5-13.5	11
Deep Depressions	> 13.5	20

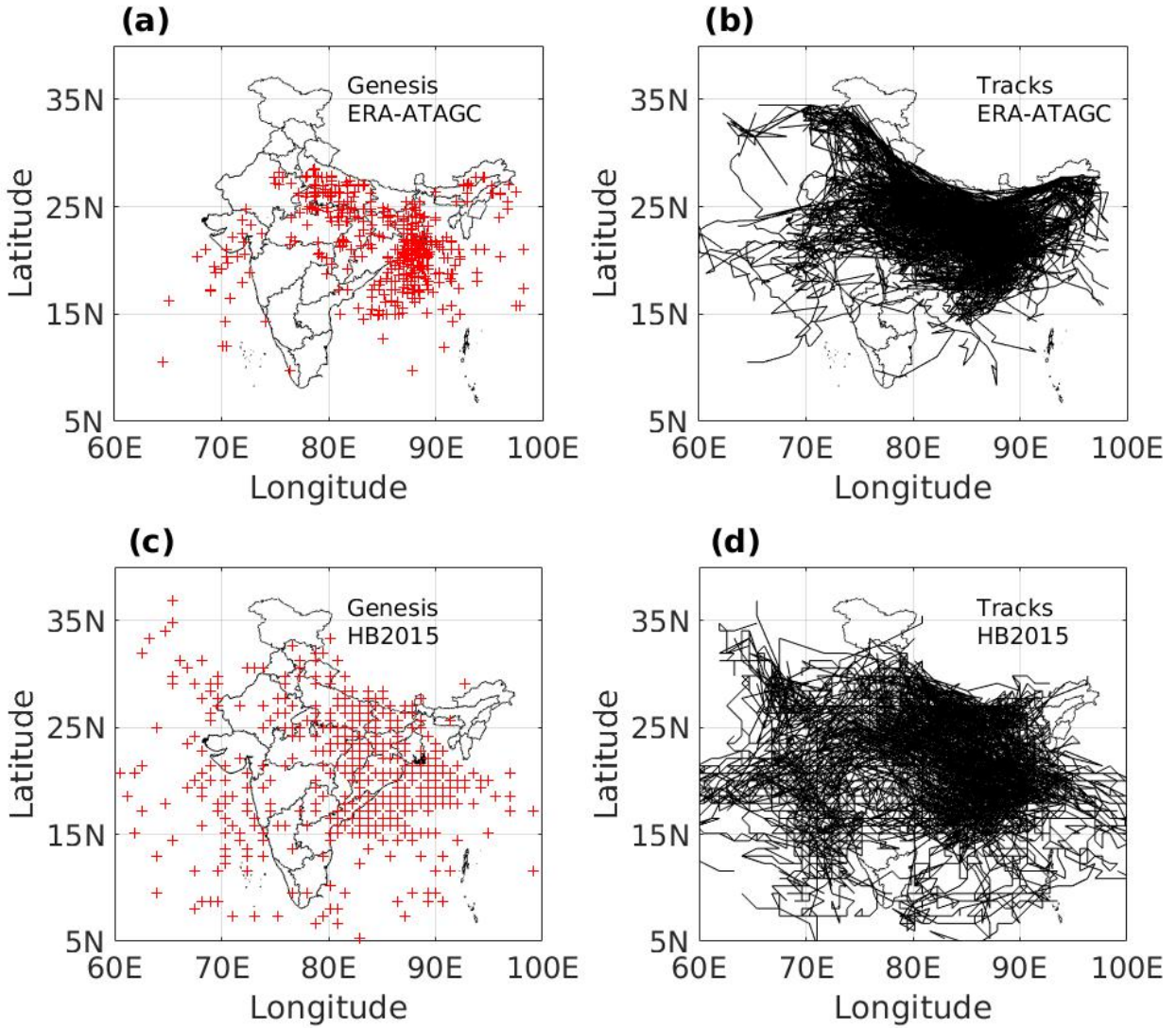


Fig. S4 LPS genesis locations (red crosses) identified by analyzing ERA-Interim data using the tracking algorithm ATAGC for the period 1979-2015 (a) and those in HB2015 for the period 1979-2012 (c). LPS tracks identified during the same period from ERA-Interim data using ATAGC (b) and in HB2015 (d). The LPS mostly form on northern BoB and move north westwards. (d) shows tracks from HB2015 which have at least one track location in the area of our study

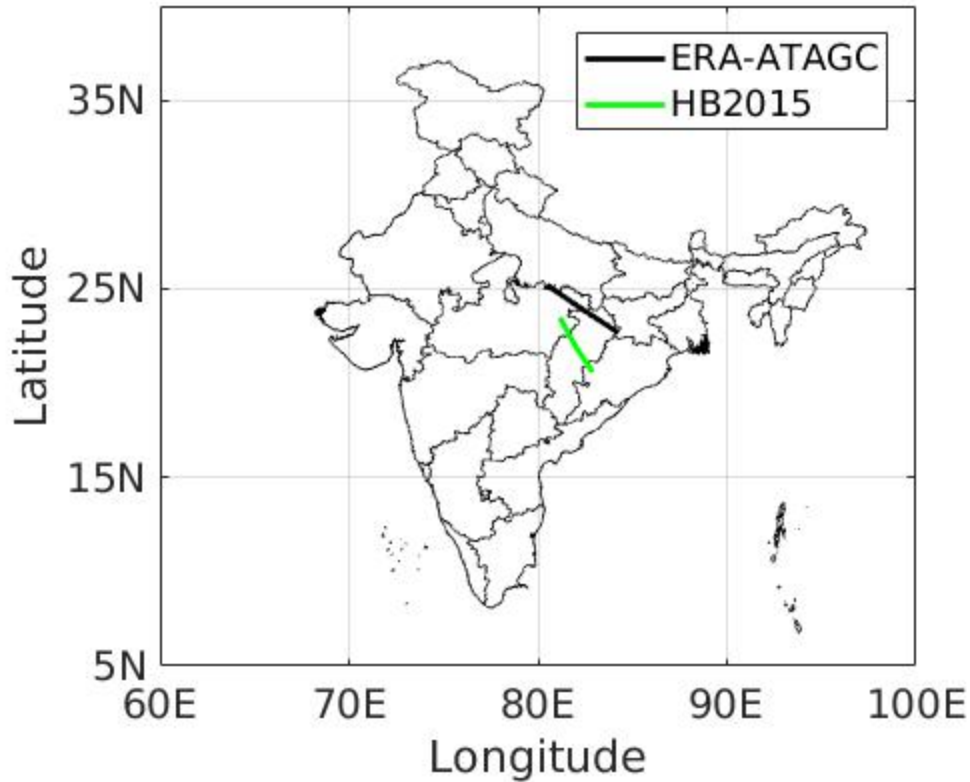


Fig. S5. Estimated lifetime axis of LPS tracks based on ATAGC during the period 1979-2015 and HB2015 tracks for the period 1979-2012. Lifetime axis is obtained by interpolating the longitudes and latitudes onto a "lifetime" axis (0.0 at genesis, 1.0 at lysis, 0.5 for the timestamp equidistant from lysis and genesis and then taking the mean). As both genesis and lysis span almost 40 degrees (60E-100E) the lifetime axis is found to be very shorter when compared to the median track constructed using the alternate method discussed in the main text shown in Fig.3.

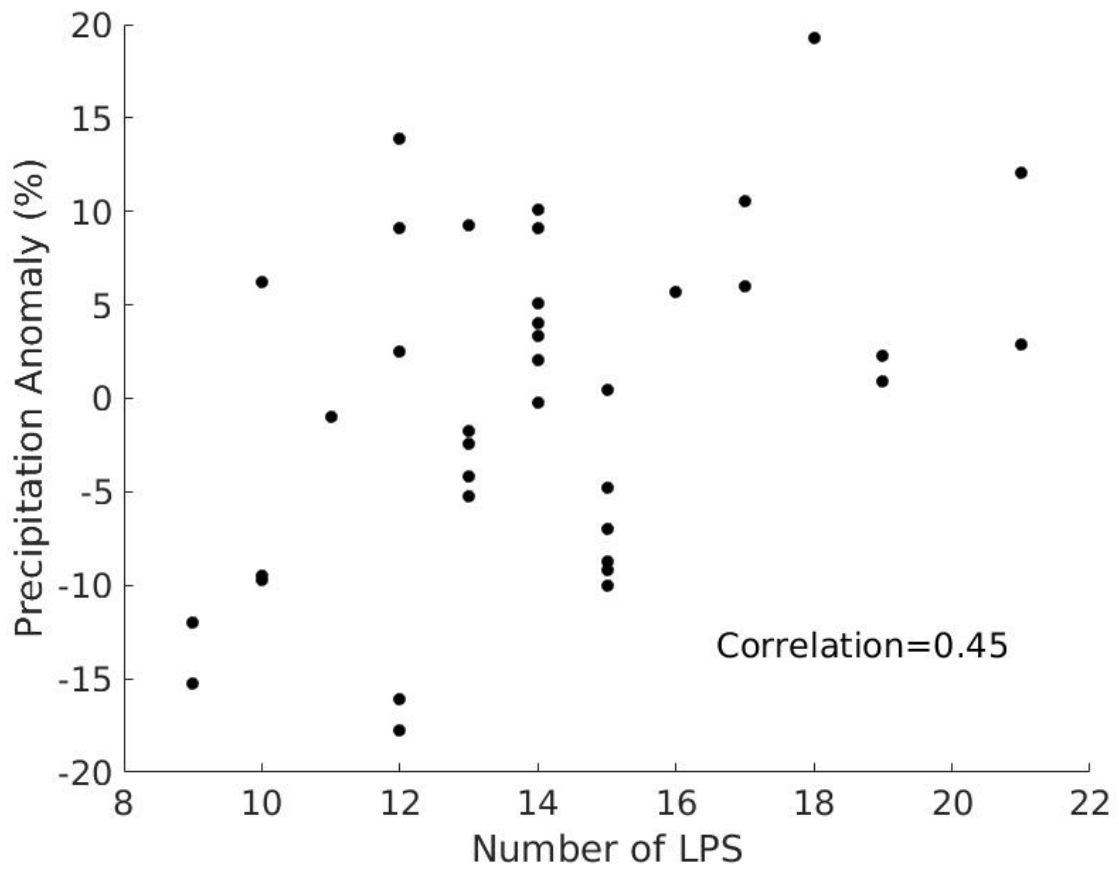


Fig. S6 Indian summer monsoon precipitation (June-September) anomaly in percentage vs annual total number of LPS in our analysis with ATAGC for the period 1979-2015.

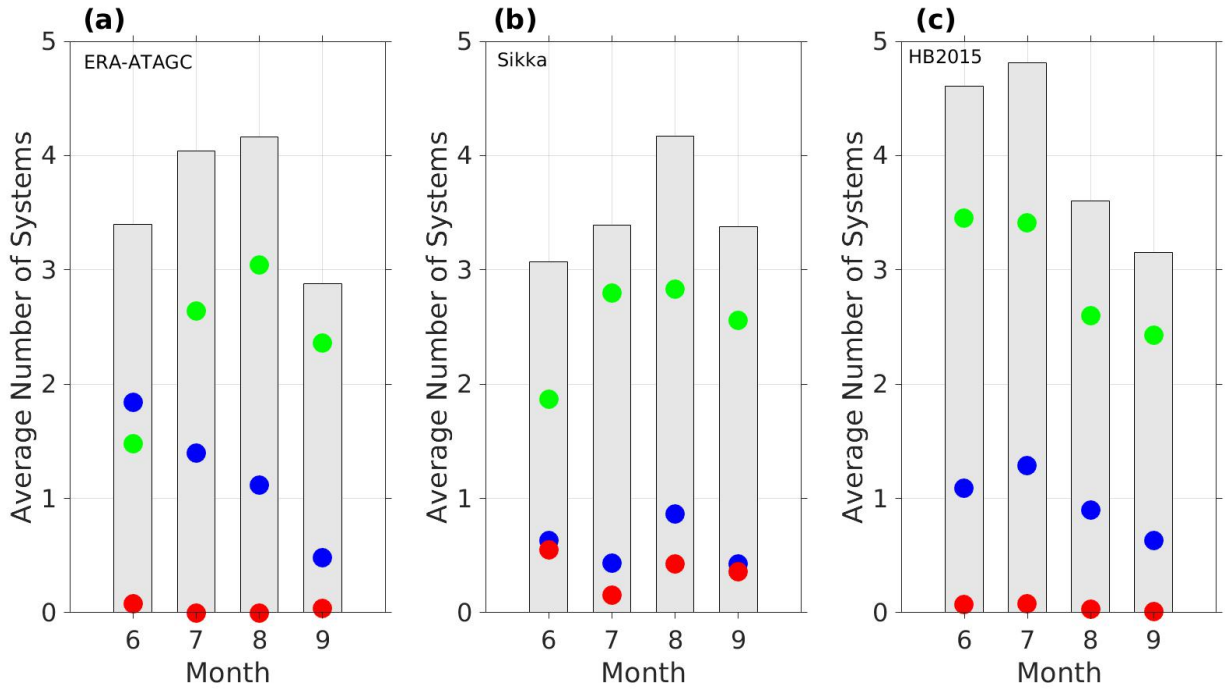


Fig. S7 Average number of different categories of LPS per year in the months of June-September for the period 1979-2003 in (a) our analysis with ATAGC on ERA-Interim data product, (b) Sikka archive and (c) HB2015. The grey bar indicates the average number of Total LPS per year and the colored dots shows the number of different categories of systems (green-Lows, blue-Depressions and red - Deep Depressions)

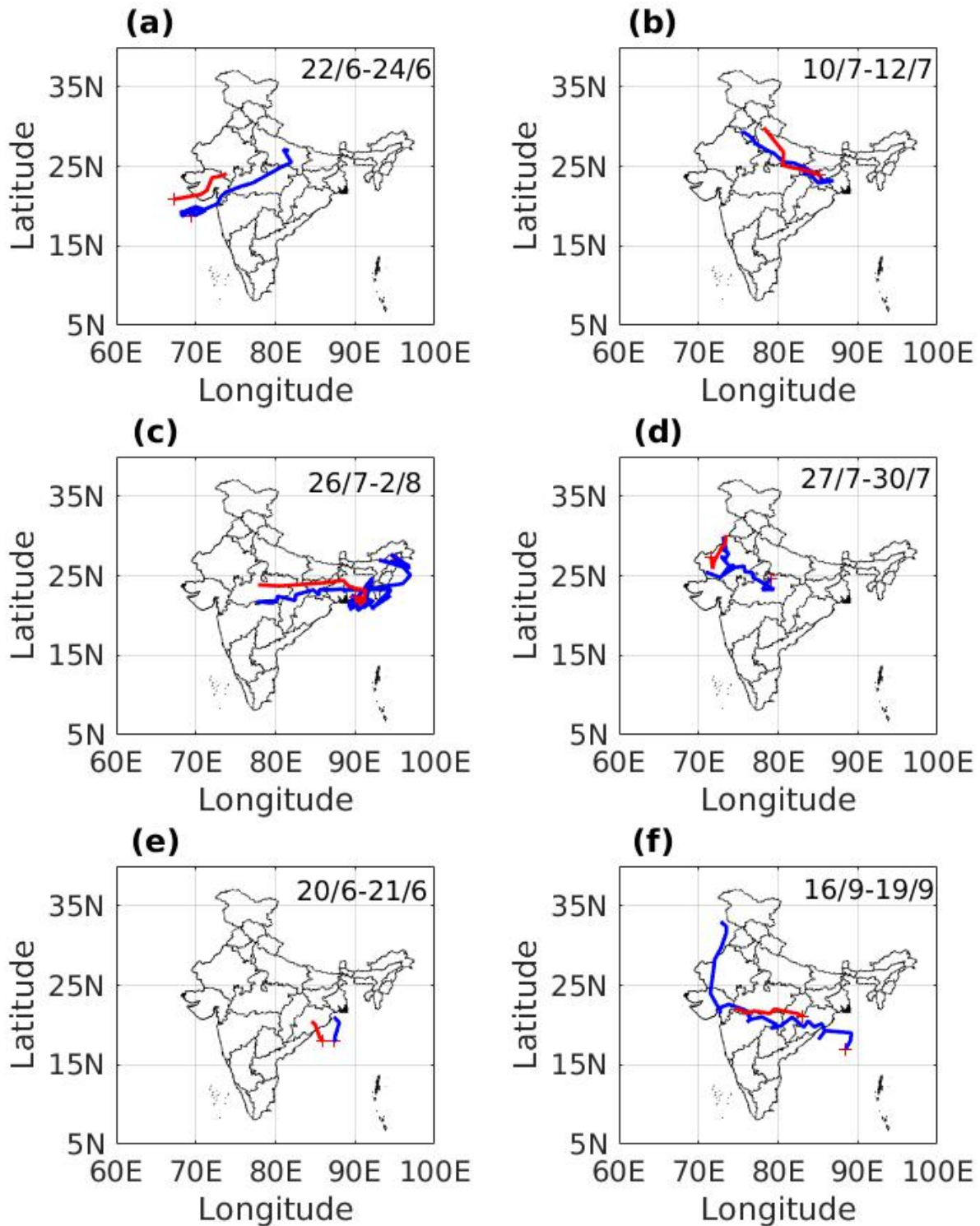


Fig. S8 Spatial comparison of tracks of the six depressions and deep depressions that are observed by IMD (IITM, 2015) and also tracked by ATAGC on ERA-Interim dataset for the year 2015. Red line represents IMD tracks and blue line represents the tracks obtained by ATAGC applied on ERA-Interim dataset. The cross symbol represents the location of genesis for the tracks

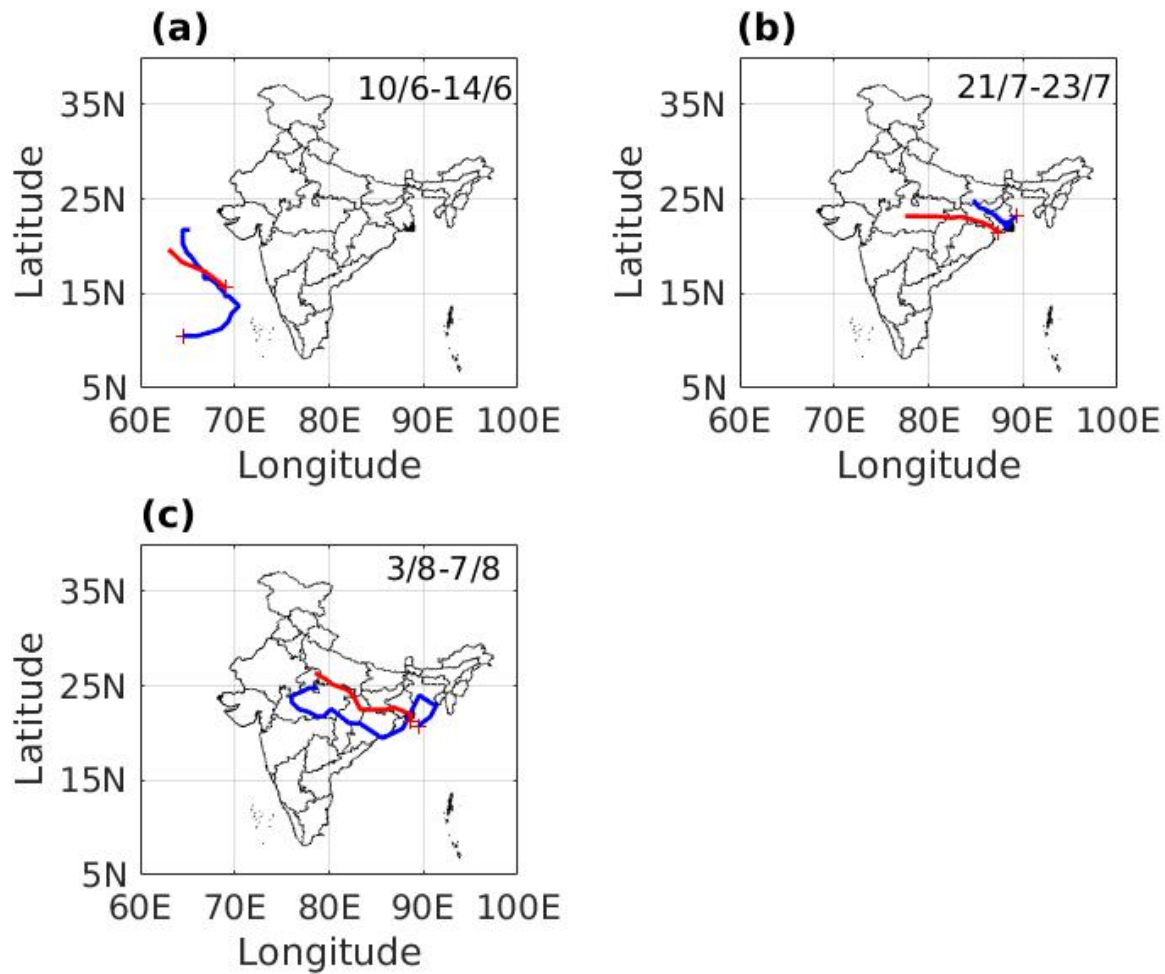


Fig. S9 Spatial comparison of tracks of the three depressions and deep depressions observed by IMD (IMD, 2015) and also tracked by ATAGC on ERA-Interim dataset for the year 2014. Red line represents IMD tracks and blue line represents the tracks obtained by ATAGC applied on ERA-Interim dataset. The cross symbol represents the location of genesis for the tracks

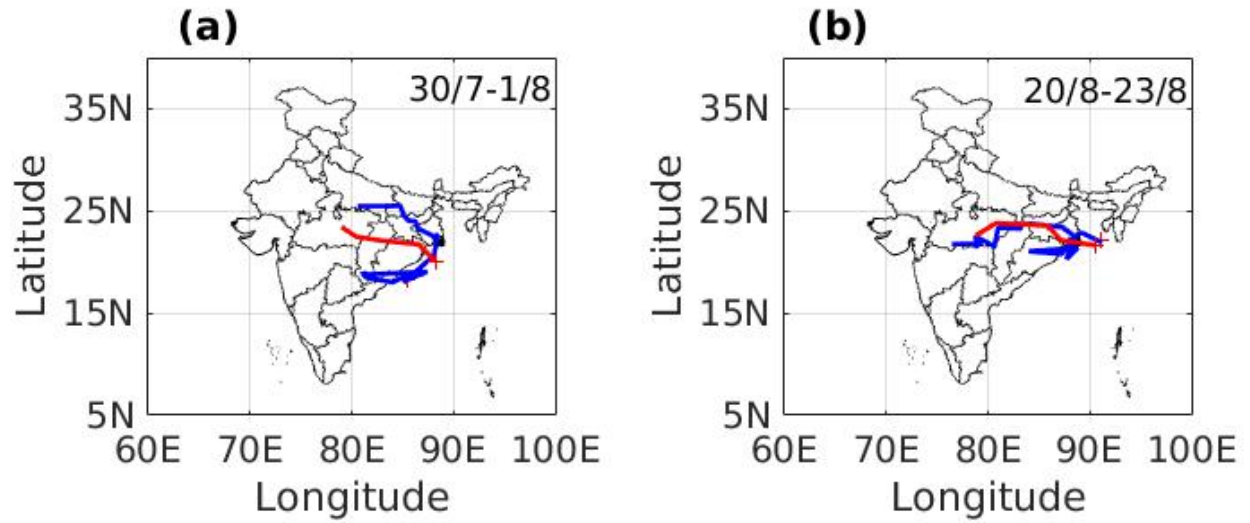


Fig. S10 Spatial comparison of tracks of the two depressions and deep depressions observed by IMD (IMD, 2014) and also tracked by ATAGC on ERA-Interim dataset for the year 2013. Red line represents IMD tracks and blue line represents the tracks obtained by ATAGC applied on ERA-Interim dataset. The cross point represents the location of genesis for the tracks

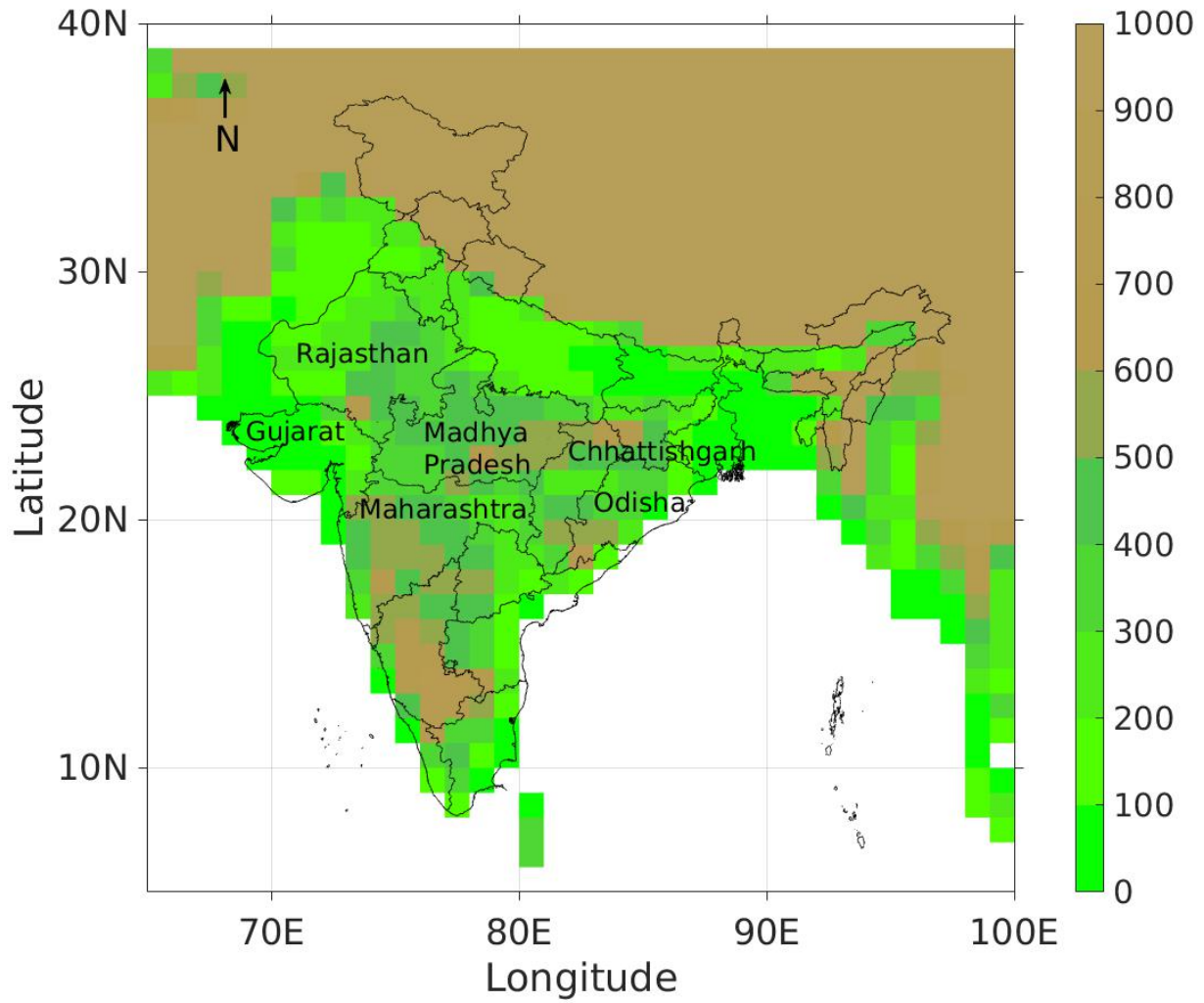


Fig. S11 Political and Topography (in meters) map of India. States which are primarily affected by LPS activity are shown

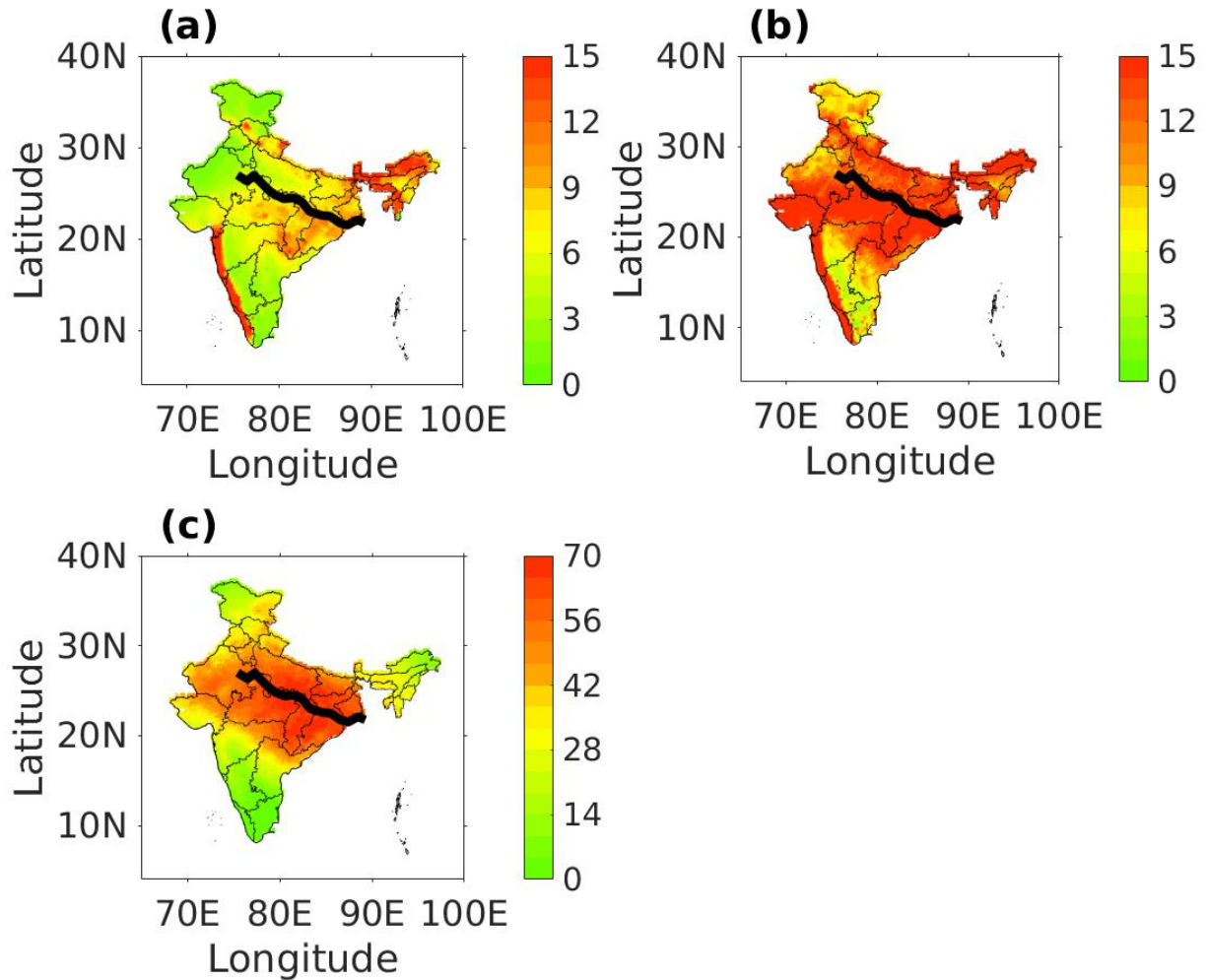


Fig. S12 Average daily precipitation during monsoon (a), within 1000km radii of ATAGC based tracks (in mm/day) (b) and percentage of LPS related precipitation to total precipitation (c) along with median track (black solid line) during monsoon over the period 1979-2015. Precipitation occurring within 1000km radii of LPS tracks is considered as LPS related precipitation. LPS tracks are obtained by applying ATAGC algorithm on ERA-Interim data, and IMD daily precipitation data ($0.25^\circ \times 0.25^\circ$ resolution) are used for precipitation analysis

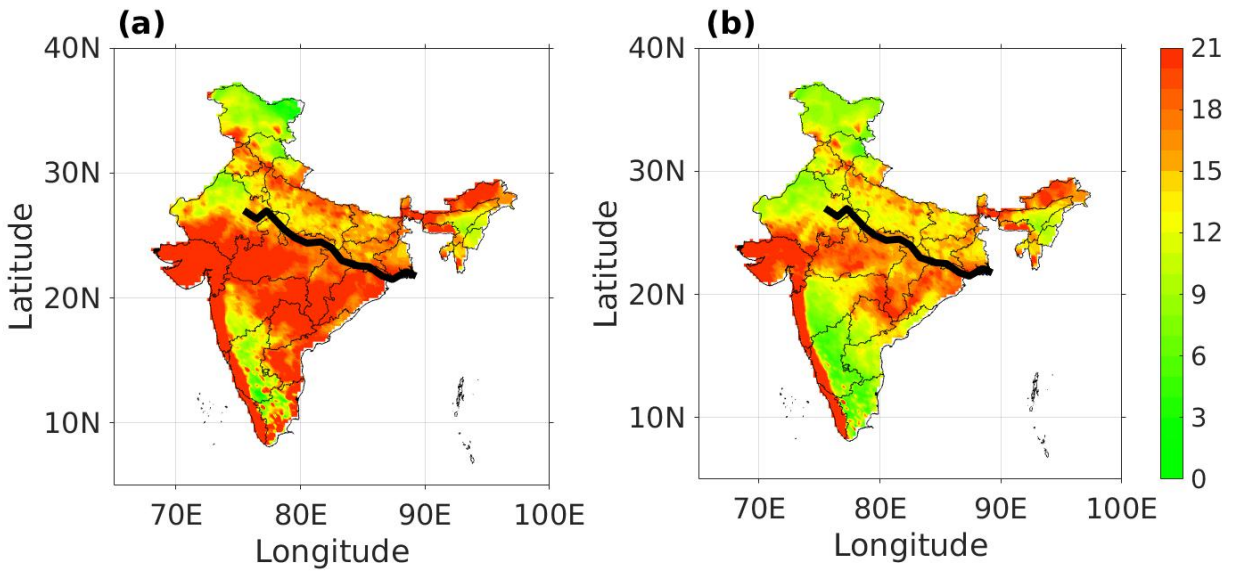


Fig. S13 Mean precipitation (in mm/day) within (a) 500km radii (b) 800km radii of ATAGC based LPS tracks along with the median track (black solid line) during the period 1979-2015. Estimates are based on daily precipitation data from IMD ($0.25^{\circ} \times 0.25^{\circ}$). The correlation between precipitation estimates based on 500km and 1000 km (Fig. 8) radii is 0.96 and that between estimates based on 800km and 1000km radii is 0.99

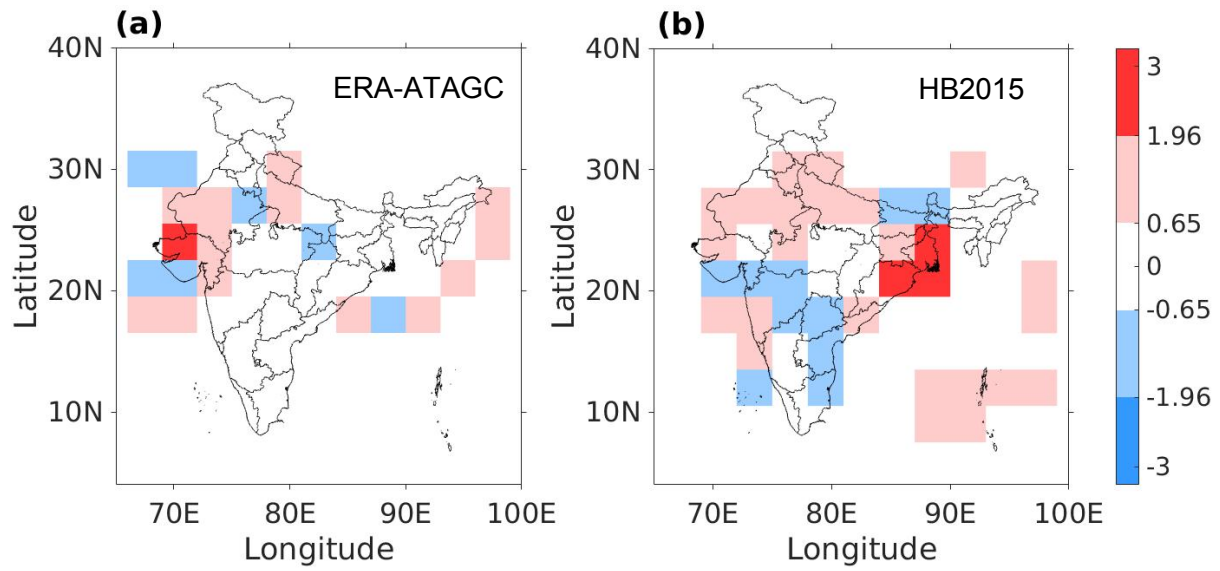


Fig. S14 Mann Kendall trend values of SAI for (a) ATAGC tracks (1979-2015) and (b) HB2015 tracks during the period 1979-2012. At 95% confidence level, trend value greater than +1.96 (or less than -1.96) is considered significant

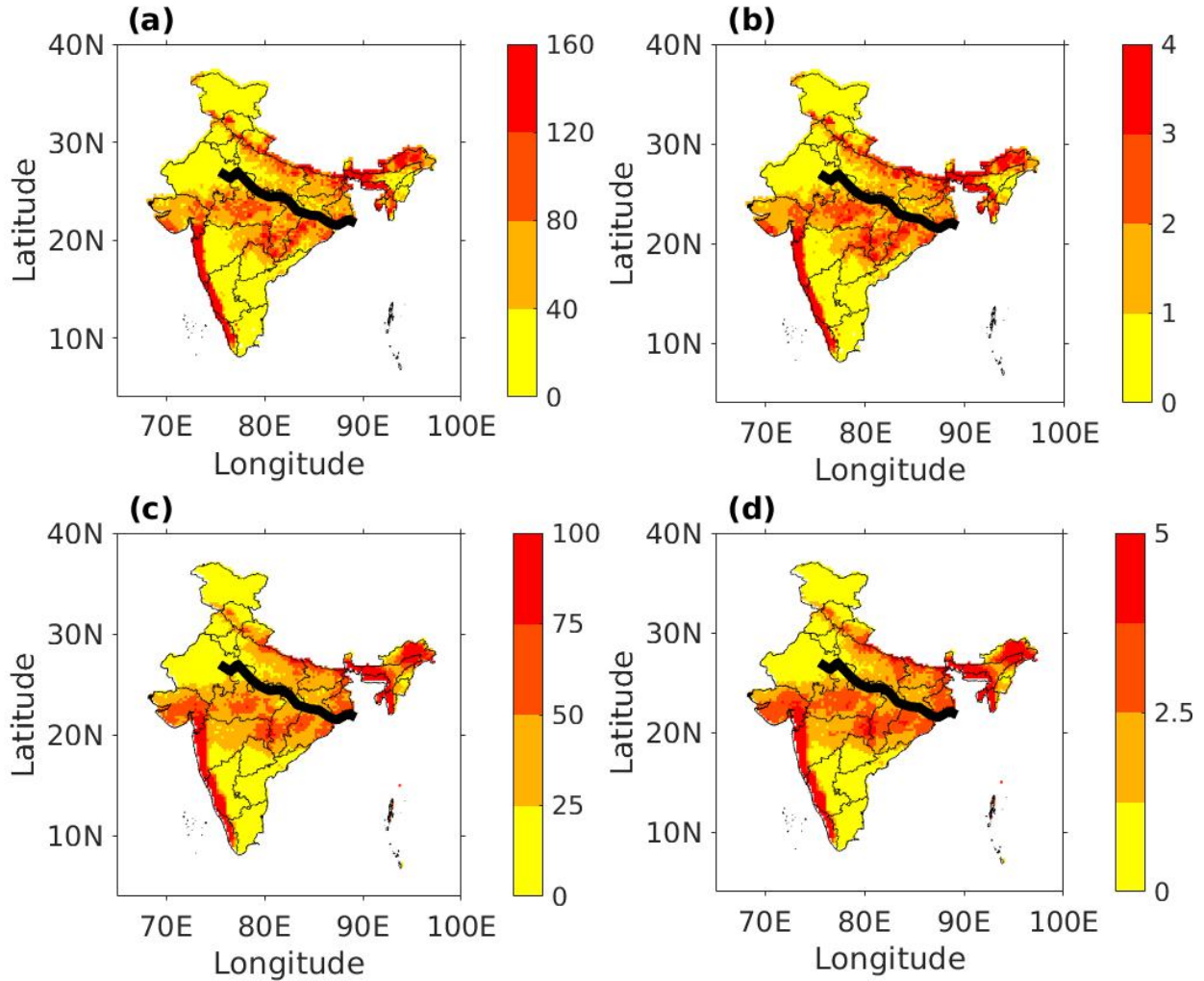


Fig. S15 (a) Number of extreme events (daily precipitation > 64.5mm) observed during 1979-2015 and (b) Annual average frequency of the extreme events during the same period estimated using daily precipitation data from IMD at 0.25°x0.25° resolution. (c) Number of extreme events during 1998-2015 and (d) Annual average frequency of extreme events during the same period estimated using daily TRMM gridded precipitation data at 0.25°x0.25° resolution. The spatial correlation between (a) and (c) is 0.87, which is the same as that between (b) and (d). The median track (black solid line) during the period 1979-2015 is obtained by applying ATAGC algorithm on ERA-Interim dataset

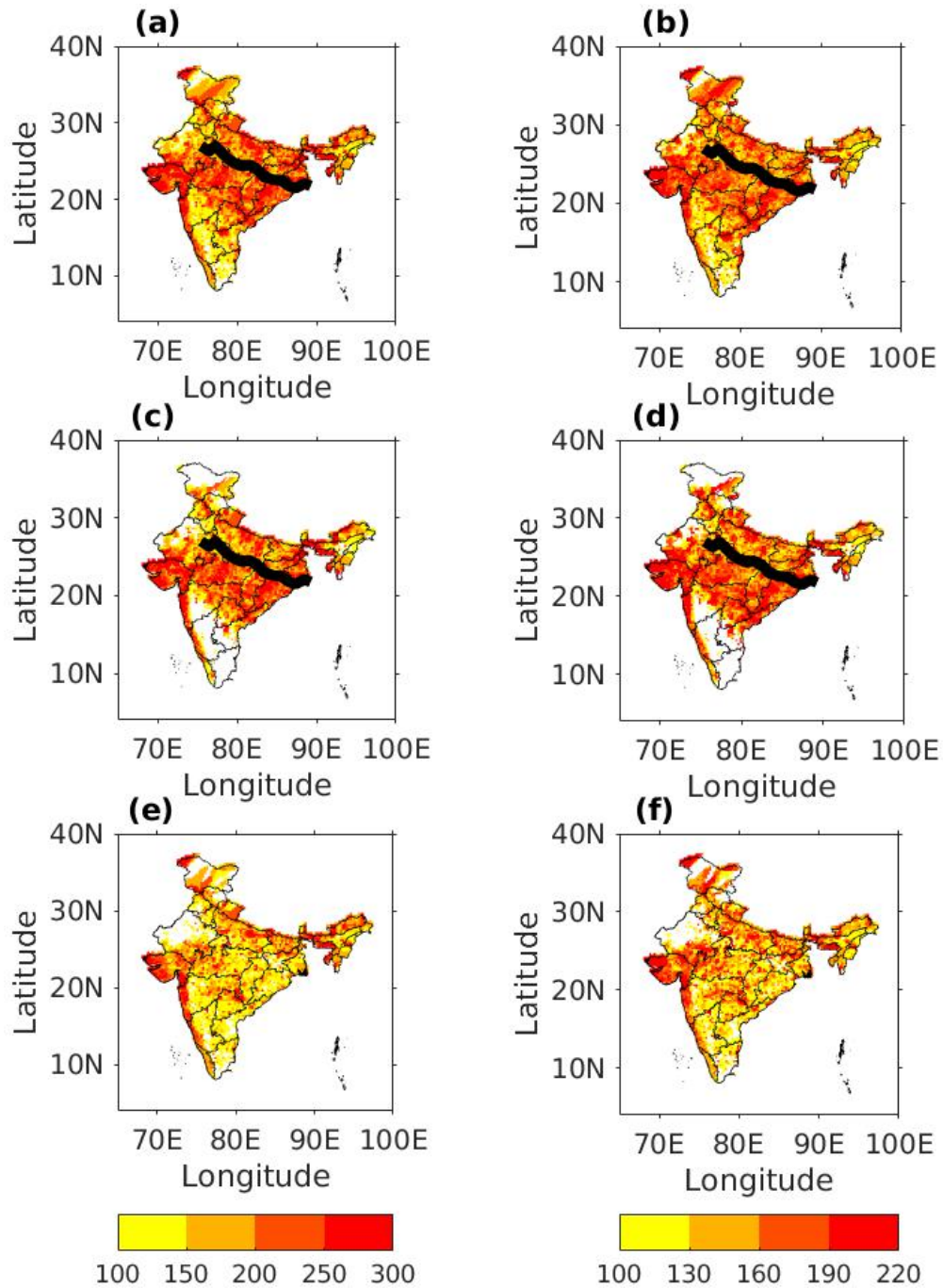


Fig. S16 The 99th percentile value (a,c,e) and 95th percentile value (b,d,f) of the extreme precipitation (mm/day) considering all extreme events (a,b), those associated with LPS (at locations within 1000km radii of LPS tracks) (c,d) along with the median track (black solid line) and those not associated with LPS (all minus those associated with LPS) (e,f) during the period 1979-2015. The LPS tracks are obtained by applying ATAGC algorithm on ERA-Interim dataset, and $0.25^{\circ} \times 0.25^{\circ}$ resolution IMD daily precipitation data are used for extreme precipitation analysis

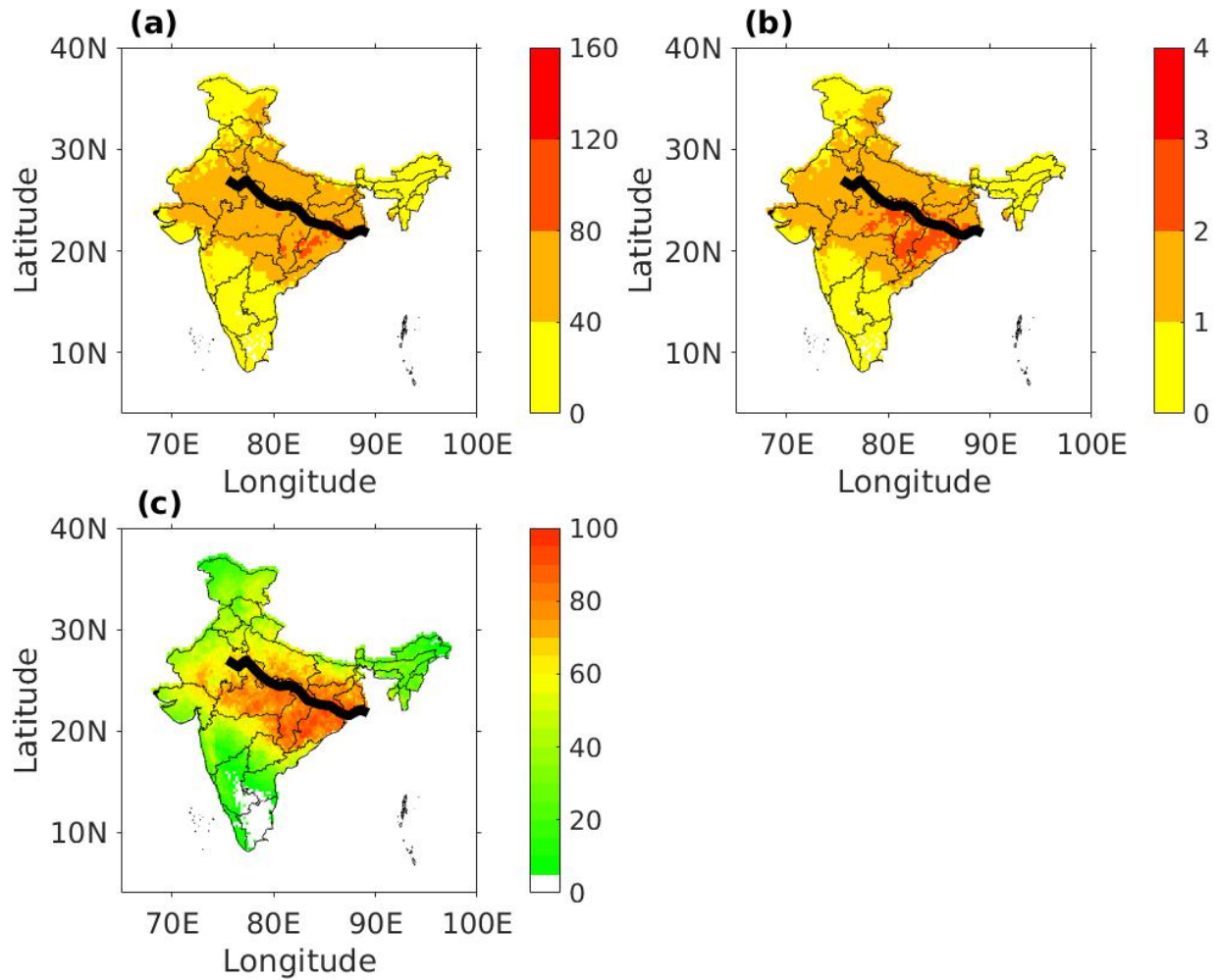


Fig. S17 Extreme precipitation events (daily precipitation larger than 98-percentile of precipitation) at grid points/locations within 1000km radii of ATAGC based LPS tracks during the period 1979-2015: (a) total count (frequency), (b) annual frequency, and (c) ratio (in %) of number of LPS-related extremes to the total number of extremes during monsoon over the period 1979-2015.

Table S2 Number of different categories of systems observed by IMD and that obtained by applying ATAGC on ERA Interim data during 2012-2015. The reasons for discrepancy are discussed in remarks

Year	IMD	ATAGC_ERA	Remark
2015	Deep Depression: 2 Depression: 6 Lows: 3	Deep Depression: 1 Depression: 5 Lows: 3	<ul style="list-style-type: none"> ● ATAGC did not count 1 deep depression with lifetime <2days in the study area. ● ATAGC classified 2 depressions as 1 depression since they occurred near each other, both in time and space.
2014	Deep Depression: 1 Depression: 2 Lows: 10	Deep Depression: 1 Depression: 8 Lows: 6	<ul style="list-style-type: none"> ● ATAGC did not count 2 lows with lifetime <2days. ● ATAGC also did not track 1 low over land and 1 low formed over southern India. ● ATAGC tracked 3 lows of IMD as 6 tracks (a combination of 2 tracks each). ● 4 lows of IMD were categorized as depressions (5 depressions) by ATAGC. ● An extra land depression and 2 lows were also tracked by ATAGC. ● Deep Depression in ATAGC analysis was categorized as tropical cyclone.
2013	Deep Depression: 0 Depression: 2 Lows: 16	Deep Depression: 0 Depression: 7 Lows: 7	<ul style="list-style-type: none"> ● ATAGC did not count 6 lows with lifetime <2days in our study area. ● ATAGC also missed to track a low of IMD over land. ● 2 lows of IMD were counted as 1 depression in the ATAGC analysis. ● 2 lows of IMD were also categorized as 3 depressions by ATAGC. ● 1 low of IMD was tracked as 2 lows by ATAGC. ● An extra depression and 2 lows over land were also tracked by ATAGC.
2012	Deep Depression: 0 Depression: 0 Lows: 10	Deep Depression: 0 Depression: 1 Lows: 12	<ul style="list-style-type: none"> ● ATAGC did not track 2 lows of duration <2days and 1 low formed over southern India. ● 1 low of IMD was tracked as 2 lows by ATAGC.

			<ul style="list-style-type: none">● 1 Low of IMD was categorized as a depression by ATAGC.● 5 extra land lows were tracked by ATAGC.
--	--	--	---

References

Ajayamohan RS, Merryfield WJ, Kharin VV (2010) Increasing trend of synoptic activity and its relationship with extreme rain events over central India. *J Climate* 23(4):1004-1013. <https://doi.org/10.1175/2009JCLI2918.1>.

Blender R, Schubert M (2000) Cyclone tracking in different spatial and temporal resolutions. *Mon Wea Rev* 128(2):377-384.

IITM M ESSO (2015) A research report on the 2015 southwest monsoon. ISSN 0252-1075, ESSO/IITM/SERP/SR/02(2015)/185:23-33.

IMD (2011) Monsoon 2010. IMD Met Monograph. Synoptic Meteorology No: 10/2011:21-47.

IMD (2012) Monsoon 2011. IMD Met Monograph. Synoptic Meteorology No: 01/2012:17-30.

IMD (2013) Monsoon 2012. IMD Met Monograph. Synoptic Meteorology No: 13/2013:15-46.

IMD (2014) Monsoon 2013. IMD Met Monograph. ESSO Document No:ESSO/IMD/Synoptic Met./01(2014)/15:10-13.

IMD. (2015) Monsoon 2014. IMD Met Monograph. ESSO Document No:ESSO/IMD/Synoptic Met./01(2015)/17:08-13.